Malaysian Journal of Chemistry, 2021, Vol. 23(4), 66-76
(Special Issue: 17th Asian Symposium on Medicinal Plants and Spices (ASOMPS XVII)
August 17-19th 2021 – Virtual Conference)

Site of Metabolism (SOM) Predictions for *Centella asiatica* and *Orthosiphon stamineus* Marker Compounds with CYP3A4 Using a Molecular Docking Approach

Mohamad Jemain Mohamad Ridhwan[1,2], Syahrul Imran Abu Bakar[1,2*] and Nor Hadiani Ismail[1,2]
[1]Faculty of Applied Sciences, Universiti Teknologi MARA (UiTM), Shah Alam, Selangor, Malaysia
[2]Atta-ur-Rahman Institute for Natural Products Discovery, Universiti Teknologi MARA (UiTM), Puncak Alam, Selangor, Malaysia
*Correspondence author (e-mail: syahrulimran@uitm.edu.my)

The human liver enzyme CYP3A4 plays an important role in the biotransformation of xenobiotics from herbs to harmless and excretable metabolites. However, CYP3A4 catalytic activity may also produce more toxic metabolites. Predicting sites of metabolism (SOMs) in the xenobiotics may prevent unwanted CYP3A4 products. The evidence to explain the comprehensive biotransformation of major compounds from *Centella asiatica* and *Orthosiphon stamineus* is inadequate. The aim of the present study was to determine the specific interaction between CYP3A4 ferric-oxidative active sites and potential SOMs for the major chemical compounds of *C. asiatica* and *O. stamineus*. Molecular docking on CYP3A4 ferric-oxo (bound to the protoporphirin group, HEME–Fe^{3+}–O^{-}) was carried out using the CDOCKER simulation program to predict the SOMs for compounds from *C. asiatica* (asiaticoside, madecassoside, asiatic acid and madecassic acid) and *O. stamineus* (sinensetin, eupatorin and 5-hydroxy-6,7,3',4'-tetramethoxyflavone (5TMF)). Binding energies, residue–ligand interactions, and SOMs were obtained from the analysis. The molecular docking results also revealed that sinensetin, eupatorin, and 5TMF bound strongly to the CYP3A4 active site with binding energies of -22.44, -34.29, and -25.84 kcal/mol, respectively. Generally, the residues Arg106, Ile301, Ther309, Glu374 and Ala307 were identified to have the highest number of interactions with eupatorine, 5TMF and sinensetin. The SOM prediction for eupatorine showed interactions between the oxygen of the HEME iron (ferric-oxo) and the C-11 and O-4 atoms. The possible metabolism reactions were C-11-hydroxylation and O-4-demethylation. For 5TMF, the SOM prediction for interactions were at the C-13 and O-7 positions, which could undergo hydroxylation and *O*-demethylation reactions, respectively. The SOM of sinensetin was predicted at C-3' and the possible metabolic reaction taking place would be hydroxylation. The present study concluded that the major compounds of *O. stamineus* have the potential to be metabolized by CYP3A4 through hydroxylation and *O*-demethylation reactions. These data may be useful for phytomedicine product development related to CYP3A4 biotransformation mechanisms.

Key words: CYP3A4; biotransformation; site of metabolism; *Centella asiatica*; *Orthosiphon stamineus*

Received: October 2021; Accepted: November 2021

Metabolism plays an essential role in toxicology because the bioactivity of toxicants can be enhanced or decreased by this process. These metabolic reactions are catalyzed by enzymes through various pathways. Understanding an enzyme's catalytic mechanism is incredibly important for drug discovery and can reduce the likelihood of problems caused by toxicokinetic issues [1]. The metabolism of human xenobiotics consists of two phases (phase I and phase II) which inactivate and convert nonpolar compounds into polar metabolites. Metabolites are excreted through either urine or bile to avoid toxic effects from accumulation of nonpolar xenobiotics in the body. However, more toxic, reactive or carcinogenic metabolites can also be produced during the biotransformation process. The metabolism of xenobiotics derived from herbs has become a major concern in current research due to the increased demand for herbal products as an effective treatment for various diseases as well as to investigate safety issues related to the consumption of herbal products.

Centella asiatica (Umbelliferare) and *Orthosiphon stamineus* (Lamiaceae) are common traditional medicinal plants used by Malaysians to treat many diseases. These herbs are grown widely in

†Paper presented at the 17th Asian Symposium on Medicinal Plants and Spices (ASOMPS XVII) August 17-19th 2021 – Virtual Conference

South Asian countries and can easily be found in Malaysia [2-3]. An abundance of health products based on these herbs are available in the market in the form of teas, tonics, juices, coffee, pills, and capsules. The *in vitro* and *in vivo* studies of crude extracts, fractions and pure compounds derived from these herbs have demonstrated promising results for a wide range of bioactivities with different mechanisms of action. Most of the therapeutic activities are attributed to secondary metabolites like terpenoids and flavones. *C. asiatica* contains large amounts of asiatic acid, madecassic acid, asiaticoside, and madecassoside [4]. In contrast, sinensetin, eupatorin and 5-hydroxy-6,7,3',4'-tetramethoxyflavone (5TMF) of poly-methoxylated flavones are the major compounds found in *O. stamineus* [5]. The major compounds in both these herbs have been proven to exhibit multiple pharmacological activities but the metabolism mechanisms of these compounds by cytochrome P450 remains unclear, especially with CYP3A4.

The metabolism of herbal xenobiotics by the human hepatic cytochrome P450 is an important metabolism pathway to detoxify herb metabolites from the body and to prevent herb-drug interactions. CYP3A4 is one of the major cytochrome P450 enzymes that is mostly expressed in the liver (approximately 28%) compared to other CYPs, and it metabolizes about 50% of active pharmaceutical ingredients [6]. The general principle of the CYP3A4 enzyme's mechanism involves introducing hydroxyl or epoxy groups to form a polar metabolite that is ready to be eliminated through the nephrons. To identify and elucidate the chemical structures of CYP3A4 metabolites, *in vitro* and *in vivo* experiments must be conducted, and these are challenging, time-consuming and involve costly study designs. Alternatively, there has been a growing focus on using molecular docking tools to predict the metabolism of the potential substrate [1, 7]. The prediction defines the site of metabolism (SOM) as well as the interaction between substrates and the oxygenated iron of HEME in the active site of CYP3A4. The results of SOM predictions using a molecular docking-based strategy can provide valuable information on the parts of the substrate that are likely to be metabolized by the enzyme. This information can also assist in the structural modification of substrates to avoid unwanted metabolic reactions.

To date, specific CYP3A4 experiments on metabolite production from the major compounds of *C. asiatica* (asiatic acid, madecassic acid, asiaticoside and madecassoside) and *O. stamineus* (sinensetin, eupatorin and 5TMF) have not been reported. Thus, the current study tries to identify the major compounds as potential substrates by demonstrating their interactions with CYP3A4 proteins via a molecular docking approach. Subsequently, SOMs for the major compounds were also predicted. The optimized CYP3A4 protein model was applied in this docking simulation using the CDOCKER program to enable fast, accurate and reliable prediction of SOMs for the major compounds.

EXPERIMENTAL

The molecular docking experiment was conducted using a slightly modified protein crystal structure of CYP3A4 complexed with ketoconazole (PDB ID: 2V0M) [8-9]. The ligands used in this investigation were four major compounds from *C. asiatica* and three known compounds from *O. stamineus* as reported in previous literature [10-12]. The molecular docking simulation was performed using the CDOCKER module in Discovery Studio 2016 software. PyMol was utilized to visualize the three-dimensional binding orientations.

1. Ligand Preparation

The two-dimensional structures of the major compounds from *C. asiatica* (asiatic acid, madecassic acid, asiaticoside and madecassoside) and *O. stamineus* (sinensetin, eupatorin and 5TMF) were prepared using ChemDraw Ultra 12.0. The ligands were then assigned using Chemistry at Harvard Macromolecular Mechanics (CHARMM) force fields in Discovery Studio software. The ligands were minimized using smart minimizer algorithms with 2000 steepest descent steps and an RMS gradient of 0.01 kcal/mol.

2. Protein Preparation

The three-dimensional protein structure of CYP3A4 bound to the ligand of ketoconazole (PDB ID: 2V0M) was retrieved from PDB (https://www.rcsb.org/pdb/home/home.do). The selection of PDB ID 2V0M in SOM molecular docking-based studies was based on the fact that the native ligand (ketoconazole) was a CYP3A4 substrate and well known as a potent inhibitor that is widely used as a positive control in CYP3A4 *in vitro* and *in vivo* inhibition experiments [13-14]. Furthermore, the size of the binding pockets in the protein structure is large enough to accommodate compounds of various sizes [15-16]. The active site provides enough space for the potential ligand to undergo dynamic structural changes and form protein-ligand interactions during molecular docking experiments [17]. Side chain A of the protein structure was used. The unwanted complexes that bound to the protein, as well as the native ligand and water molecules, were removed. The missing residues (Met23–Ser29, Thr264–Arg268, Asn280–Lys288 and Thr499–His507) and hydrogen atoms were added to the protein structure. Finally, oxygen was added to the iron of HEME to form ferric-oxo (Fe^{3+}–O^{-}).

3. Active Site Identification

Identification of CYP3A4 active sites for the selected PDB entries was conducted using Discovery Studio 2016. The active site residues (Phe57, Leu210, Phe241,

Ile301, Phe304, Ala370, Arg372, Gly481, Leu482, HEME1499) and grid coordinates (X: 18.740861, Y: 9.237028, Z: 62.003444) were identified by referring to the native ligand (ketoconazole) as well as a literature survey [15]. A sphere was generated through the centroid of the native ligand. A radius size of 15 Å was selected to provide adequate space in the active site for protein-ligand interactions and to accommodate ligands of various sizes.

4. Molecular Docking Protocol Validation

The molecular docking method was validated by re-docking the native ligand to the target protein's active site using the CDOCKER program.

5. Molecular Docking Using CDOCKER

Molecular docking was conducted using the CDOCKER module. The default settings applied to the docking parameters included: CHARMM forcefield, 10 diverse top poses, 0.1 post cluster radius, 10 random conformations, 10000 dynamic steps, 1000 °C dynamic target temperature, electrostatic interaction, 10 orientation to refine (800 bad maximum orientations, 300 orientation vender walls energy threshold) and simulated annealing (2000 heating steps, 700 °C heating target temperature, 5000 cooling steps, 300 °C cooling target temperature). The docking was implemented by maintaining protein rigidness and retaining ligand flexibility. The binding energies, protein-ligand interactions and SOMs were determined and visualized using Discovery Studio 2016 and PyMol.

RESULTS AND DISCUSSION

1. Validation of the Modified CYP3A4 Protein Structure Model Through a Molecular Docking Approach (CDOCKER)

Molecular docking was performed to investigate Protein-ligand interactions and SOMs for seven major compounds from *C. asiatica* and *O. stamineus* as CYP3A4 substrates. The basis of the docking model in a SOM study is to express the ability of a ligand to fit into a protein's active site, as well as to estimate the binding affinity and the interactions between atoms of the ligand molecule with oxygen from the HEME iron (ferric-oxo species). The CDOCKER module was used to dock major compounds of *C. asiatica* and *O. stamineus*. The module offers fast, highly efficient docking algorithms, is user friendly, and provides enhanced accuracy and reliability of results. The validation of the CDOCKER program for the SOM molecular docking-based model was conducted to assess the ability of CDOCKER to reproduce the binding mode of the native ligand in the CYP3A4 protein's active site. In this study, the native ligand was ketoconazole, a well-known CYP3A4 inhibitor. Many CYP3A4 studies have used this compound as a positive control to investigate drug-drug interactions with new molecular entities that are substrates of CYP3A4 [14, 18]. Ketoconazole is also a CYP3A4 substrate. The predominant metabolite from this compound with CYP3A4 is *N*-deacetyl-ketoconazole [13, 19-20].

Figure 1 shows the interactions between ketoconazole and the CYP3A4 binding site. The residues that were able to interact with the ligand were Leu210, Leu211, Phe241, Ile301, Ala305, Thr309, Ala370, Arg372, Gly481 and Leu482. A previous study reported that ketoconazole forms major interactions with Phe215, Arg212, Leu211, Phe304, Arg372 and Arg106 residues. In contrast to that study, the present findings demonstrated interactions between two major residues (Leu211 and Arg372) and the native ligand. Forming perfect residue interactions as reported in the previous study was impossible because each docking program used different algorithms to define the active sites in protein preparation and to perform molecular docking simulations [21-22]. Upon visual inspection, various

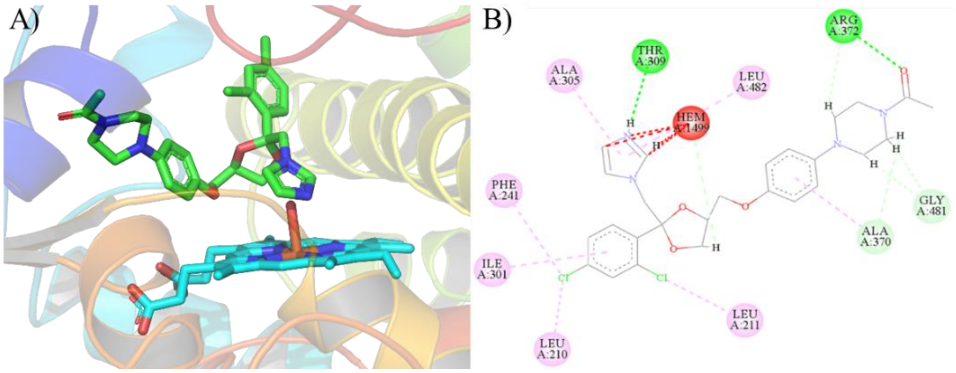

Figure 1. A) Three-dimensional molecular docking model of ketoconazole interacting with the CYP3A4 binding site and B) its two-dimensional ligand-binding residues. The crystallographic binding modes of ketoconazole are displayed as green stick carbon atoms, while ferric-oxo HEME is represented by turquoise stick carbon atoms. The colours of the dotted lines denote different interactions: carbon-hydrogen bonds (light green), conventional hydrogen bonds (dark green), alkyl interactions (light pink) and π-alkyl interactions (dark pink).

interactions were observed involving carbon- hydrogen bonding (Ala370 to C-H of a piperazine ring; Gly481 to C-H of a piperazine ring), conventional hydrogen bonding (Thr309 to N-H of an imidazole ring; Arg372 to C=O of ethanone), alkyl interactions (Leu210, Leu211 and Phe241 to C-Cl of a chlorobenzyl ring) and π-alkyl interactions (Ile301, and Ala370 to a phenyl ring; Ala305 and Leu482 to an imidazole ring). The validation results of the CYP3A4 protein-ketoconazole interactions showed that the CDOCKER module was able to correctly position the native ligand in the active site.

Figure 2 shows the superimposition of ketoconazole on the CYP3A4 crystallographic structure and the best docking conformation. The RMSD value generated from the superimposition of the native ligand and the docked structure was 1.13 Å. The RMSD value commonly applied to validate the superimposition is typically less than 2 Å [23]. Thus, the present RMSD value indicates that CDOCKER algorithm used in this research is valid and able to accurately predict the ketoconazole binding orientation. In addition, the SOM of the native ligand and the distance between the known metabolism site of ketoconazole with the ferric-oxo species were investigated, as shown in Figure 3. The metabolic reaction of ketoconazole by CYP3A4 produced *N*-deacetyl-ketoconazole. The oxidative metabolism took place on a nitrogen atom of the piperazine ring. The modified CYP3A4 protein model, with the help of the CDOCKER module, was able to accurately predict the SOM for ketoconazole (Figure 3). The distance between the targeted SOM and the oxygen from the HEME iron (ferric-oxo) was 1.22 Å which was within the acceptable distance of up to 6 Å [24-26]. This optimal docking program was used to identify the SOMs for major compounds of *C. asiatica* and *O. stamineus*.

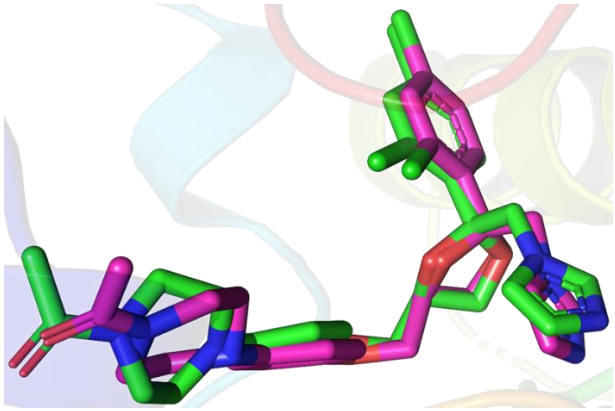

Figure 2. Ketoconazole re-docking superimposed on the native ligand of 2V0M. The crystallographic binding modes of the native ligand are displayed as pink stick carbon atoms, while the binding modes predicted are rendered as green stick carbon atoms.

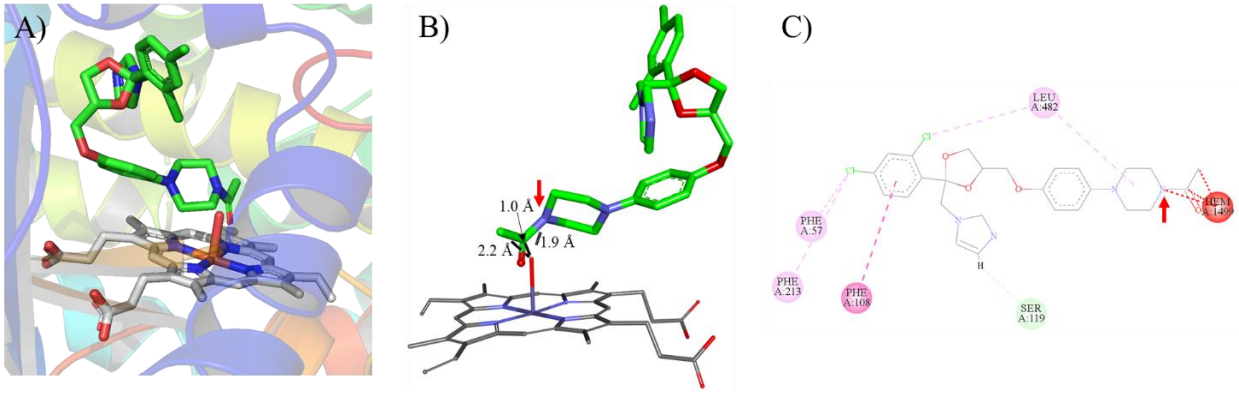

Figure 3. The SOM prediction of the ketoconazole interaction with the oxygen of the HEME iron. A) three-dimensional visualization protein-ligand interaction, B) SOM distance, and C) two-dimensional SOM interaction. Red arrows represent predicted SOMs. The crystallographic binding modes of ketoconazole are displayed as green stick carbon atoms, while ferric-oxo of HEME is shown as turquoise stick carbon atoms. The colours of the dotted lines denote various interactions: carbon-hydrogen bonds (light green), conventional hydrogen bonds (dark green) and π-alkyl interactions (light pink).

Table 1. Binding energy and residue interactions for the major compounds in *C. asiatica* and *O. stamineus*.

Ligands	Binding energy (kcal/mol)	Residue interaction			
		Carbon-hydrogen	Conventional hydrogen	Alkyl	π-alkyl
Asiatic acid	48.57	Nil	Nil	Nil	Nil
Madecassic acid	54.67	Nil	Nil	Nil	Nil
Asiaticoside	-	Nil	Nil	Nil	Nil
Madecassoside	-	Nil	Nil	Nil	Nil
Eupatorin	-34.29	Arg106, Ile301 and Thr309	Ala370	Nil	Nil
5TMF	-25.84	Arg105, Arg106 and Thr309	Glu374	Nil	Ala370
Sinensetin	-22.44	Ile301	Nil	Nil	Leu482
Ketoconazole (native ligand)	-28.23	Ala370 and Gly481	Leu210, Leu 211 and Phe241	Thr309 and Arg372	Ile301, Ala370, Ala305 and Leu482

- ligands failed to dock. Nil represents not available.

2. Molecular Docking Analysis of the Major Compounds from *C. asiatica* and *O. stamineus*

In this study, the major compounds were docked against the optimized CYP3A4 protein structure. The docking results provided a list of potential major compounds that successfully bound to the protein's active site and their binding affinities, which are shown in Table 1. Three compounds from *O. stamineus* (eupatorin, 5TMF and sinensetin) and two compounds from *C. asiatica* (asiatic acid and madecassic acid) successfully formed complexes with the CYP3A4 protein structures. The remaining two compounds, asiaticoside and madecassoside, failed to interact with the protein's active site. Binding energy is the primary parameter used to assess the strength and affinity between a ligand and a protein. Lower binding energy means higher affinity of the ligand towards the active site [27].

The protein-ligand interactions of eupatorin, 5TMF and sinensetin which passed the SOM molecular docking-based analysis are visualized in Figure 4. Eupatorin demonstrated a prominent CYP3A4 protein-ligand interaction with a binding energy of -34.29 kcal/mol. The interaction involved three carbon-hydrogen bonds (Arg106, Ile301, and Thr309 to C-H of methoxy groups), one conventional hydrogen bond (Glu374 to C-H of methoxy group) and one π-alkyl interaction (Ala370 to heterocyclic pyran ring). A desirable bond between 5TMF and the CYP3A4 protein structure was observed with a binding energy of -25.84 kcal/mol. This compound showed three carbon-hydrogen bonds (Arg105, Arg106 and Thr309 to C-H of a methoxy group), one conventional hydrogen bond (Glu374 to C-H of a methoxy group) and one π-alkyl interaction (Ala370 to a benzenic B ring). Sinensetin, with a binding energy of -22.44 kcal/mol, formed a hydrogen bond with Ile301 (C=O of a heterocyclic pyran ring) and a π-alkyl interaction with Ala482 of a benzenic B ring.

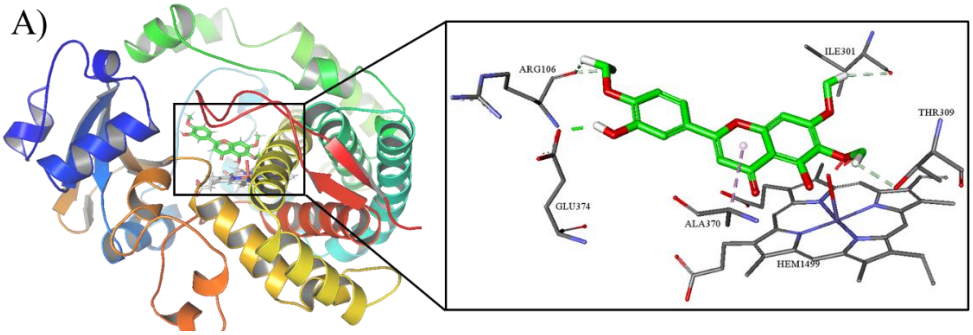

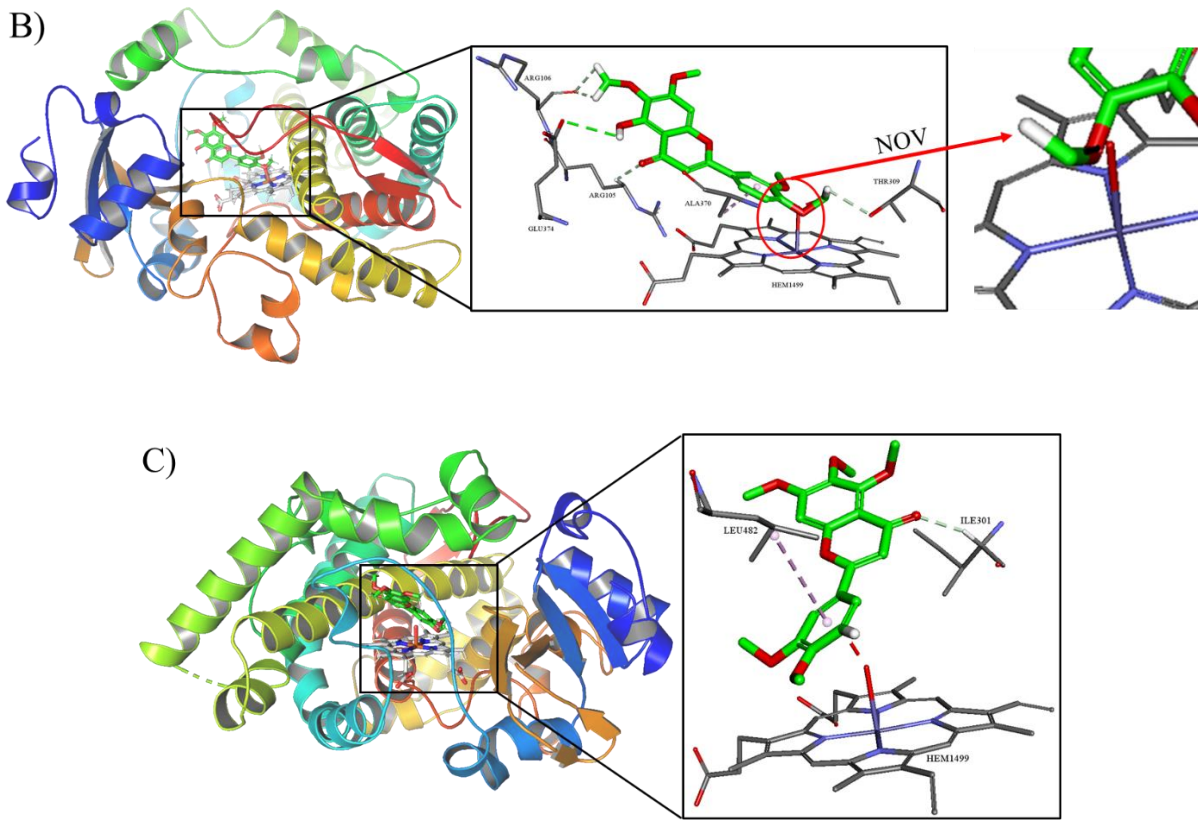

Figure 4. Three-dimensional visualization of SOM molecular docking-based results: Interaction between CYP3A4 protein with A) eupatorine B) 5TMF and C) sinensetin. The colours of the dotted lines denote various interactions: carbon-hydrogen bonds (light green), conventional hydrogen bonds (dark green) and π-alkyl interactions (light pink). NOV represents an atom of a ligand that does not overlap with the oxygen of the HEME iron.

According to the molecular docking findings, eupatorin had the lowest binding energy, indicating the highest binding affinity for protein-ligand interactions compared to other major compounds. Eupatorin also demonstrated greater binding affinity than the native ligand (ketoconazole) with a binding energy of -28.23 kcal/mol. 5TMF displayed the second highest binding energy, followed by sinensetin. In general, the residues involved in interactions with the major compounds of *O. stamineus* were Arg105, Arg106, Ile301, Thr309, Ala370, Glu374 and Leu482 (Figure 3). The residues that frequently interacted with eupatorin, 5TMF and sinensetin were Arg106, Ile 301, Thr309 and Ala307. The interactions involved either hydrophilic residues (Arg106, Ile 301 and Thr309) or hydrophobic residues (Ala307). Ala307 is one of the essential residues that plays a part in the binding of the substrate and inhibitor to the CYP3A4 active cavity and is responsible for protein structure flexibility [28]. In addition, the methoxy groups and benzene B ring of specific functional groups in the major compounds were observed as hotspots for residue interactions. Hydrogen bonding interactions were found between the residues and the C-H of methoxy groups. The benzene B rings formed π-alkyl interactions with hydrophobic residues like Ala307.

The major compounds from *O. stamineus* have the potential to interact with the CYP3A4 protein. These findings are in line with previous reports, which demonstrated that the crude extract of *O. stamineus* inhibited CYP3A4 catalytic activity through *in vitro* assays with IC_{50} values ranging from 46.30 to 97.82 µg/ml [29-31]. A previous study [29] pointed out that dichloromethane and petroleum ether extracts of this herb moderately inhibited CYP3A4 through non-competitive inhibition and mixed inhibition (*Ki* values were 44.9 and 93.7 µg/ml), respectively. They also revealed that eupatorin and sinensetin showed inhibitory activity against the human cDNA-expressed CYP3A4 enzyme. Therefore, these previous studies provide evidence that the major compounds in *O. stamineus* can form interactions with the CYP3A4 protein structure and inhibit enzyme catalytic activity. Numerous studies have proved that CYP3A4 inhibitors such as ketoconazole, erythromycin, and ritonavir can be metabolized by the same enzyme [13, 32-35].

Asiatic acid and madecassic acid demonstrated poor binding affinity towards the CYP3A4 active site with interaction energies of 48.57 and 54.67 kcal/mol, respectively. The positive values correspond to an unfavorable formation of the protein-ligand complex,

which requires energy input for a non-spontaneous reaction to occur [36]. This study found that the major compounds of *C. asiatica* formed unfavourable interactions with the CYP3A4 protein active site, in contrast with previous studies. A previous molecular docking study [6] showed a strong binding interaction (-70.07 kcal/mol) between asiaticoside and the CYP3A4 protein structure obtained from a protein data bank (PDB ID: 4NY4) for the purpose of investigating CYP3A4 inhibitors. Inhibitory activities of the major compounds of *C. asiatica* towards recombinant human CYP3A4 were investigated and the results demonstrated that these compounds inhibited the enzyme [37-39]. However, this study failed to identify the protein-ligand interactions of the major compounds due to possible protein-ligand clashes and larger ligands trying to enter the small cavities of CYP3A4 [40].

3. Site of Metabolism (SOM) Predictions for Major Compounds of *O. stamineus*

All three ligands from *O. stamineus* (eupatorin, 5MTF and sinensetin) formed favourable interactions with residues in the CYP3A4 active site. The molecular docking results of the ligands were further examined to rationalize the ligands as potential CYP3A4 substrates via observation of their SOMs. The results in Table 2 show the distances between the predicted SOM and the oxygen of the HEME iron, which indicate that the SOMs of eupatorin, 5TMF, and sinensetin were successfully predicted with interaction distances between the ligand atom and the oxygen of the HEME iron in the range of 0.58 to 2.20 Å. The reactive oxygen of the HEME iron mostly interacted with the ligand's carbon and oxygen atoms and the major compounds of *O. stamineus*. The molecular docking studies defined the interaction of SOMs as steric interactions. A factor contributing to cytochrome P450's metabolic responsibility of SOMs is steric accessibility of the target atom to a substrate that is controlled by the hydrogen abstraction energy in carbon oxidation at the final phase of the catalytic cycle [41-42]. The oxygen from the ferric-oxo HEME was transferred to the substrate, resulting in a hydroxylated product characterized as a polar metabolite [43-45]. In addition, the present study tried to mimic the final phase of the CYP3A4 metabolism mechanism as closely as possible by producing a modified version of the CYP3A4 protein model which was employed in the molecular docking analysis to predict SOMs.

The SOM prediction for eupatorin showed that the C-11 and O-4 of methoxy groups can interact with the oxygen of the HEME iron at a distance of 2.00 and 1.74 Å, respectively (Figure 5). The two-dimensional docked structure of eupatorin and CYP3A4 demonstrated that the hydrogen atoms from the methoxy groups (C-6, C-7 and C-4') and the hydroxyl group (C-3') formed hydrogen bonds with Arg106, Ile301, Thr309 and Glu374 residues. Another residue, Ala370, formed a π-alkyl interaction with a heterocyclic pyran ring to further stabilize the protein-ligand complex. The residues of Arg106 (in a B-C loop), Ile301 and Thr309 (both in a Helix I loop) were located in the flexible loop of the CYP3A4 structure [46-47]. The flexibility of these binding residues (Arg106, Ile301 and Thr309) assisted in the positioning the methoxy group of eupatorin close to the ferric-oxo of HEME. Based on the molecular docking results, it was possible for SOMs for eupatorin to go through hydroxylation (C-11) and *O*-demethylation (O-4).

Table 2. Prediction of SOMs for the major compounds in *C. asiatica* and *O. stamineus* by molecular docking in the CYP3A4 protein structure.

Compounds	Predicted SOM	Distance of SOM (Å)	Predicted metabolism reaction
Asiatic acid	No SOM	Nil	Nil
Madecassic acid	No SOM	Nil	Nil
Asiaticoside	No SOM	Nil	Nil
Madecassoside	No SOM	Nil	Nil
Eupatorin	C-11	2.00	Hydroxylation
	O-4	1.74	*O*-demethylation
5TMF	C-13	1.50	Hydroxylation
	O-7	0.58	*O*-demethylation
Sinensetin	C-3'	2.20	Hydroxylation

SOM represents site of metabolism. Nil represents not available.

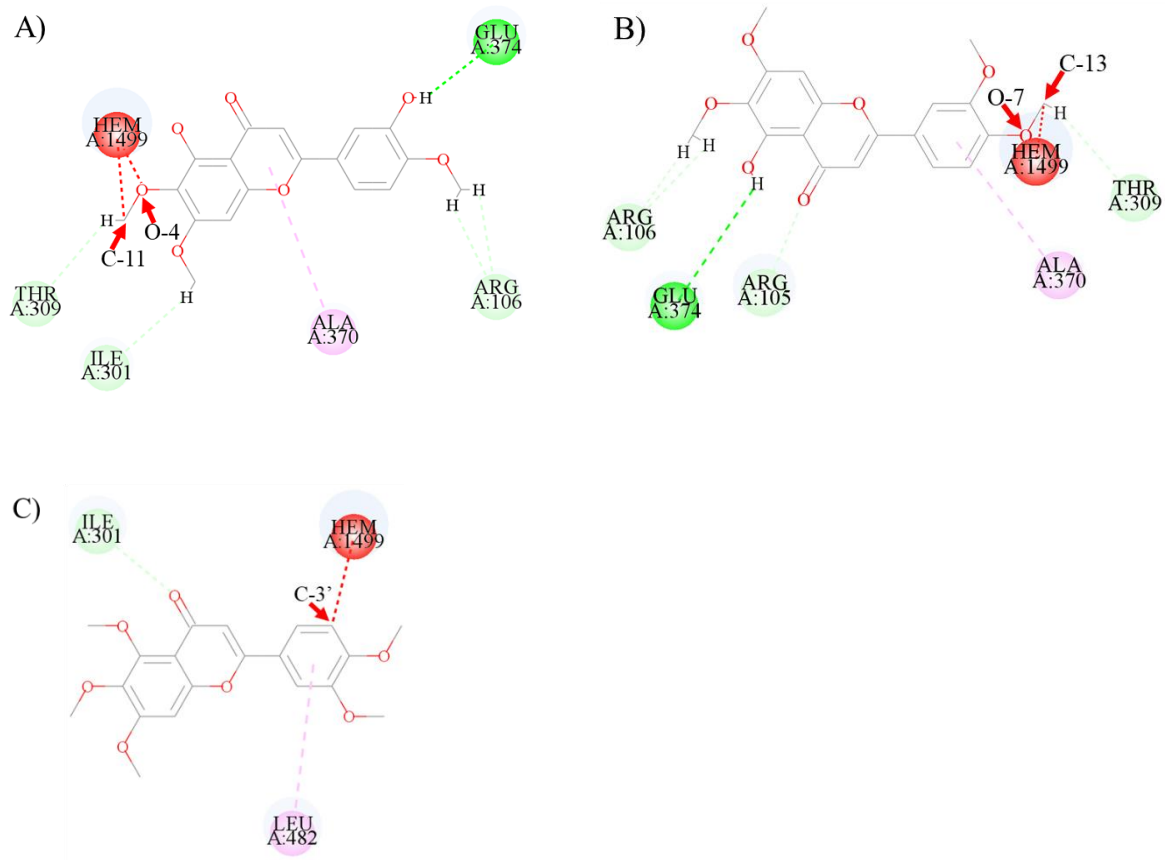

Figure 5. Two-dimensional visualization of SOM predictions: CYP3A4 residues-ligand interactions for A) eupatorin, B) 5TMF and C) sinensetin. The colours of the dotted lines denote various interactions: carbon-hydrogen bonds (light green), conventional hydrogen bonds (dark green) and π-alkyl interactions (light pink). Red arrows represent SOMs.

For 5TMF, the C-13 and O-7 of the methoxy group were able to form SOM interactions with the oxygen of HEME at a distance of 1.50 and 0.58 Å, respectively (Figure 5). The stable protein-ligand complex could be due to the hydrogen bonding and π-alkyl interactions with Arg105, Arg106, Thr309, Glu374 and Ala370. The molecular docking analysis of the protein-ligand complex found that the methoxy (C-6 and C-4'), hydroxyl group (C-5) and carbonyl (C-4) of 5TMF could form hydrogen bonds with Arg105, Arg106, Thr309 and Glu374 residues. The complex was further stabilized through a π-alkyl interaction between the heterocyclic pyran ring and the Ala370 residue. Arg105, Arg106 (both in a B-C loop), Thr309 (both in a Helix I loop) residues positioned in the flexible loops of the CYP3A4 structure were essential to orientate the SOM of 5TMF close to the oxygen of the HEME iron. Possible reactions that could take place at the SOM of 5TMF were *O*-demethylation (O-7) and hydroxylation (C-13).

The molecular docking analysis also predicted CYP3A4 SOM for siensetin at the C-3' of the benzene B ring with a distance of 2.20 Å from the oxygen of the HEME iron (Figure 5). The two-dimensional docking results showed that two residues were responsible to stabilize and position the ligand close to the reactive oxygen of the HEME iron in the active site. Ile301 formed hydrogen bonds with C-4 of the carbonyl group, while Leu482 formed a π-alkyl interaction with the benzene B ring. Both Ile301 (in a Helix I loop) and Leu482 (in a C terminal loop) residues were identified as essential residues in the flexible loop of the CYP3A4 protein. The proposed catalytic reaction at the predicted SOM of sinensetin was hydroxylation (C-3') due to the SOM interaction forming at the C-H of the benzene ring.

The overall SOM results revealed that the major compounds of *O. stamenues* (eupatorin, 5TMF and sinensetin) have the potential to be metabolized by CYP3A4. The SOM interactions between flavone-type compounds and the oxygen of HEME point to the methoxy groups (eupatorin and 5TMF) and the benzene B ring (sinensetin). CYP34A was able to metabolize some flavone compounds through the main metabolic routes involving hydroxylation on the benzene rings and *O*-demethylation in the methoxy groups. A previous *in vitro* CYP3A4 study showed that the SOM of nobeletin was located at the 6- and 7-position of the methoxy group, resulting in the production of 6-hydroxynobelatin and 7-hydroxnobeletin through an *O*-demethylation reaction [48]. Another flavone metabolism study found that a catalytic hydroxylation reaction by mammalian

CYP3A4 had taken place on benzene rings B and C of naringin and naringenin [49]. Hence, the findings of these two studies indicated that eupatorin, 5TMF and sinensetin had potential to be used as CYP3A4 substrates.

Aside from the prediction of SOMs, the molecular docking analysis also showed essential residue interactions with the ligand active sites. The observation of the predicted SOM for each ligand found that one active residue interacted near the SOM. Thr309 formed interactions with methoxy groups of eupatorin and 5TMF. A similar finding was observed for sinensetin, in which the SOM prediction and Leu482 interacted at the same benzene ring B. Both these residues were identified as key residues responsible for substrate binding, cooperativity and regioselectivity of CYP3A4 metabolism [22, 47].

CONCLUSIONS

In this study, site of metabolism (SOM) molecular docking-based predictions were made for the major compounds in *C. asiatica* (asiatic acid, madecassic acid, asiaticoside and madecassoside) and *O. stamineus* (eupatorin, 5TMF and sinensetin) against a modified CYP3A4 protein structure. All major compounds of *O. stamineus* favourably interacted with CYP3A4's active site. Eupatorin had a better binding interaction compared to the native ligand, ketoconazole. The major compounds of *C. asiatica* were unable to interact with the CYP3A4 protein structure. Further observations of the docked protein-ligand complex structures found that the interactions of SOMs were as follows: C-11 and O-4 of the methoxy group for eupatorin, C-13 and O-7 of the methoxy group for 5TMF, and C-3' of the benzene B ring for sinensetin. The hydrogen bonding and π-alkyl interactions with Arg105, Arg106, Thr309, Glu374 and Ala370 residues may have played a part in stabilizing and orientating the ligands into the right position. These major compounds of *O. stamineus* show potential as CYP3A4 substrates and thus provide a new research direction for metabolic pathways that lead to safe and effective therapeutic applications of these herbs.

DISCLOSURE

No potential conflict of interest was reported by the authors.

ACKNOWLEDGEMENTS

The authors gratefully acknowledge Ministry of Health Malaysia (MOH) and Atta-ur-Rahman Institute for Natural Products Discovery for providing outstanding laboratory facilities. The authors would also like to thank Universiti Teknologi MARA Malaysia for financial support through the Young Talent Researcher Grant 600-RMC/YTR/5/3 (008/2021). The authors would like to acknowledge the Malaysian Ministry of Higher Education (KPT) for the financial support under FRGS Grant File No. 600-IRMI/ FRGS 5/3 (111/2019).

REFERNCES

1. Tyzack, J. D. and Kirchmair, J. (2019) Computational methods and tools to predict cytochrome P450 metabolism for drug discovery. *Chemical Biology & Drug Design*, **93(4)**, 377–386.

2. Ameer, O. Z., Salman, I. M., Asmawi, M. Z., Ibraheem, Z. O. and Yam, M. F. (2012) *Orthosiphon stamineus*: traditional uses, phytochemistry, pharmacology, and toxicology. *Journal of Medicinal Food*, **15(8)**, 678–90.

3. Alfarra, H. Y. and Omar, M. N. (2013) *Centella asiatica*: from folk remedy to the medicinal biotechnology - a state revision. *International Journal of Biosciences*, **3**, 49–67.

4. Gray, N. E., Alcazar Magana, A., Lak, P., Wright, K. M., Quinn, J., Stevens, J. F., Maier, C. S. and Soumyanath, A. (2018) *Centella asiatica* - Phytochemistry and mechanisms of neuroprotection and cognitive enhancement. *Phytochemistry reviews : proceedings of the Phytochemical Society of Europe*, **17(1)**, 161–194.

5. Deipenbrock, M. and Hensel, A. (2019) Polymethoxylated flavones from *Orthosiphon stamineus* leaves as antiadhesive compounds against uropathogenic E. coli. *Fitoterapia*, **139**, 104387.

6. Ashour, M. L., Youssef, F. S., Gad, H. A. and Wink, M. (2017) Inhibition of cytochrome P450 (CYP3A4) activity by extracts from 57 plants used in traditional chinese medicine (TCM). *Pharmacognosy Magazine*, **13(50)**, 300–308.

7. Wang, Y., Xing, J., Xu, Y., Zhou, N., Peng, J., Xiong, Z., Liu, X., Luo, X., Luo, C., Chen, K., Zheng, M. and Jiang, H. (2015) *In silico* ADME/T modelling for rational drug design. *Quarterly Reviews of Biophysics*, **48(4)**, 488–515.

8. Scior, T. and Quiroga, I. (2019) Induced fit for cytochrome P450 3A4 based on molecular dynamics. *ADMET and DMPK*, **7(4)**, 252.

9. Nair, P. C., McKinnon, R. A. and Miners, J. O. (2019) Computational Prediction of the Site(s) of Metabolism and Binding Modes of Protein Kinase Inhibitors Metabolized by CYP3A4. *Drug Metabolism and Disposition*, **47(6)**, 616.

10. Hoss, M. and Ismail, Z. (2011) New prenylated flavonoids of *Orthosiphon stamineus* grown in

Malaysia. *Asian Journal of Biotechnology*, **3(2)**, 200–205.

11. Hossain, M. A. and Mizanur Rahman, S. M. (2015) Isolation and characterisation of flavonoids from the leaves of medicinal plant *Orthosiphon stamineus*. *Arabian Journal of Chemistry*, **8(2)**, 218–221.

12. Sun, B., Wu, L., Wu, Y., Zhang, C., Qin, L., Hayashi, M., Kudo, M., Gao, M. and Liu, T. (2020) Therapeutic potential of *Centella asiatica* and its triterpenes: A Review. *Frontiers in Pharmacology*, **11**, 568032.

13. Kim, J.-H., Choi, W.-G., Lee, S. and Lee, H. S. (2017) Revisiting the metabolism and bioactivation of ketoconazole in human and mouse using liquid chromatography-mass spectrometry-based metabolomics. *International Journal of Molecular Sciences*, **18(3)**, 621.

14. Yang, L., Yan, C., Zhang, F., Jiang, B., Gao, S., Liang, Y., Huang, L. and Chen, W. (2018) Effects of ketoconazole on cyclophosphamide metabolism: evaluation of CYP3A4 inhibition effect using the *in vitro* and *in vivo* models. *Experimental animals*, **67(1)**, 71–82.

15. Ekroos, M. and Sjögren, T. (2006) Structural basis for ligand promiscuity in cytochrome P450 3A4. *Proceedings of the National Academy of Sciences*, **103(37)**, 13682.

16. Müller, C. S. (2014) Functional investigations of cytochrome P450 3A4. ETH Zurich.

17. Ohkura, K., Kawaguchi, Y., Watanabe, Y., Masubuchi, Y., Shinohara, Y. and Hori, H. (2009) Flexible structure of cytochrome P450: promiscuity of ligand binding in the CYP3A4 heme pocket. *Anticancer research*, **29(3)**, 935–942.

18. Yang, L., Feng, J., Zhang, F., Jiang, B., Gao, S. and Chen, W. (2014) Fast quantification of cyclophosfamide and its N-dechloroethylated metabolite 2-dechloroethylcyclophosphamide in human plasma by UHPLC-MS/MS. *Biomedical Chromatography*, **28(10)**, 1303–1305.

19. Greenblatt, H. K. and Greenblatt, D. J. (2014) Liver injury associated with ketoconazole: review of the published evidence. *The Journal of Clinical Pharmacology*, **54(12)**, 1321–1329.

20. European Medicines Agency *Assessment report Ketoconazole HRA*; 09 September 2021, 2021.

21. Jurčík, A., Byška, J., Sochor, J. and Kozlíková, B. (2015) Visibility-based approach to surface detection of tunnels in proteins, in *Proceedings of the 31st Spring Conference on Computer Graphics*, Slovakia, **65–72**.

22. Benkaidali, L., André, F., Maouche, B., Siregar, P., Benyettou, M., Maurel, F. and Petitjean, M. (2013) Computing cavities, channels, pores and pockets in proteins from non-spherical ligands models. *Bioinformatics*, **30(6)**, 792–800.

23. Rimac, H., Grishina, M. and Potemkin, V. (2021) Use of the complementarity principle in docking procedures: A new approach for evaluating the correctness of binding poses. *Journal of Chemical Information and Modeling*, **61(4)**, 1801–1813.

24. Hritz, J., de Ruiter, A. and Oostenbrink, C. (2008) Impact of plasticity and flexibility on docking results for cytochrome P450 2D6: a combined approach of molecular dynamics and ligand docking. *Journal of Medicinal Chemistry*, **51(23)**, 7469–7477.

25. Shaik, S., Cohen, S., Wang, Y., Chen, H., Kumar, D. and Thiel, W. (2010) P450 Enzymes: Their structure, reactivity, and selectivity—modeled by QM/MM calculations. *Chemical Reviews*, **110(2)**, 949–1017.

26. Kingsley, L. J., Wilson, G. L., Essex, M. E. and Lill, M. A. (2015) Combining structure- and ligand-based approaches to improve site of metabolism prediction in CYP2C9 substrates. *Pharmaceutical Research*, **32(3)**, 986–1001.

27. Pantsar, T. and Poso, A. (2018) Binding affinity via docking: Fact and fiction. *Molecules (Basel, Switzerland)*, **23(8)**, 1899.

28. Kiani, Y. S., Ranaghan, K. E., Jabeen, I. and Mulholland, A. J. (2019) Molecular dynamics simulation framework to probe the binding hypothesis of cyp3a4 inhibitors. *International Journal of Molecular Sciences*, **20(18)**, 4468.

29. Pan, Y., Abd-Rashid, B. A., Ismail, Z., Ismail, R., Mak, J. W., Pook, P. C., Er, H. M. and Ong, C. E. (2011) *In vitro* effects of active constituents and extracts of *Orthosiphon stamineus* on the activities of three major human cDNA-expressed cytochrome P450 enzymes. *Chemico-Biological Interactions*, **190(1)**, 1–8.

30. Purwantiningsih and Hussin, A. H. (2014) Interaction study: the effect of *Orthosiphon stamineus* extract on human cytochrome P450. *Indonesian Journal of Pharmacy*, **25**, 230.

31. N. A, H., Azizi, J., Ismail, S. and Mansor, S. (2010) Evaluation of selected Malaysian medicinal plants on phase i drug metabolizing enzymes, CYP2C9, CYP2D6 and CYP3A4

activities *in vitro*. *International Journal of Pharmacology*, **6**.

32. Zhou, S. F. (2008) Drugs behave as substrates, inhibitors and inducers of human cytochrome P450 3A4. *Current Drug Metabolism*, **9(4)**, 310–22.

33. Orlando, R., Piccoli, P., De Martin, S., Padrini, R. and Palatini, P. (2003) Effect of the CYP3A4 inhibitor erythromycin on the pharmacokinetics of lignocaine and its pharmacologically active metabolites in subjects with normal and impaired liver function. *British journal of clinical pharmacology*, **55(1)**, 86–93.

34. Sevrioukova, I. F. and Poulos, T. L. (2010) Structure and mechanism of the complex between cytochrome P4503A4 and ritonavir. *Proceedings of the National Academy of Sciences of the United States of America*, **107(43)**, 18422–18427.

35. Parmentier, Y., Pothier, C., Delmas, A., Caradec, F., Trancart, M.-M., Guillet, F., Bouaita, B., Chesne, C., Brian Houston, J. and Walther, B. (2017) Direct and quantitative evaluation of the human CYP3A4 contribution (fm) to drug clearance using the *in vitro* SILENSOMES model. *Xenobiotica*, **47(7)**, 562–575.

36. Sharifi, M., Dolatabadi, J. E., Fathi, F., Rashidi, M., Jafari, B., Tajalli, H. and Rashidi, M. R. (2017) Kinetic and thermodynamic study of bovine serum albumin interaction with rifampicin using surface plasmon resonance and molecular docking methods. *Journal of Biomedical Optics*, **22(3)**, 37002.

37. Patel, K., Mishra, R. and Patel, D. K. (2016) A review on phytopharmaceutical importance of asiaticoside. *Journal of coastal life medicine*, **4**, 1000–1007.

38. Nagoor Meeran, M. F., Goyal, S. N., Suchal, K., Sharma, C., Patil, C. R. and Ojha, S. K. (2018) Pharmacological properties, molecular mechanisms, and pharmaceutical development of asiatic acid: A pentacyclic triterpenoid of therapeutic promise. *Frontiers in Pharmacology*, **9**, 892–892.

39. Pan, Y., Abd-Rashid, B. A., Ismail, Z., Ismail, R., Mak, J. W., Pook, P. C., Er, H. M. and Ong, C. E. (2010) *In vitro* modulatory effects on three major human cytochrome P450 enzymes by multiple active constituents and extracts of *Centella asiatica*. *Journal of Ethnopharmacology*, **130(2)**, 275–283.

40. Grigoryan, A., Wang, H. and Cardozo, T. (2012) Can the energy gap in the protein-ligand binding energy landscape be used as a descriptor in virtual ligand screening?. *PloS one*, **7**, e46532.

41. Liu, J., Machalz, D., Wolber, G., Sorensen, E. J. and Bureik, M. (2021) New Proluciferin Substrates for Human CYP4 Family Enzymes. *Applied Biochemistry and Biotechnology*, **193(1)**, 218–237.

42. Kirchmair, J., Göller, A. H., Lang, D., Kunze, J., Testa, B., Wilson, I. D., Glen, R. C. and Schneider, G. (2015) Predicting drug metabolism: experiment and/or computation?. *Nature Reviews Drug Discovery*, **14(6)**, 387–404.

43. Campelo, D. (2019) *Domain dynamics and control of electron flux of NADPH cytochrome P450 oxidoreductase*. Ph.D. Thesis, Universidade Nova de Lisboa, Lisbon, Portugal.

44. Guengerich, F. P. (2007) Mechanisms of cytochrome P450 substrate oxidation: MiniReview. *Journal of Biochemical and Molecular Toxicology*, **21(4)**, 163–168.

45. Prasad, B., Mah, D. J., Lewis, A. R. and Plettner, E. (2013) Water oxidation by a cytochrome p450: mechanism and function of the reaction. *PloS one*, **8(4)**, e61897.

46. Benkaidali, L., André, F., Moroy, G., Tangour, B., Maurel, F. and Petitjean, M. (2019) Four major channels detected in the cytochrome P450 3A4: A step toward understanding its multispecificity. *International Journal of Molecular Sciences*, **20(4)**, 987.

47. Sevrioukova, I. F. and Poulos, T. L. (2013) Understanding the mechanism of cytochrome P450 3A4: recent advances and remaining problems. *Dalton transactions (Cambridge, England : 2003)*, **42(9)**, 3116–3126.

48. Koga, N., Ohta, C., Kato, Y., Haraguchi, K., Endo, T., Ogawa, K., Ohta, H. and Yano, M. (2011) *In vitro* metabolism of nobiletin, a polymethoxy-flavonoid, by human liver microsomes and cytochrome P450. *Xenobiotica*, **41(11)**, 927–933.

49. Bai, Y., Peng, W., Yang, C., Zou, W., Liu, M., Wu, H., Fan, L., Li, P., Zeng, X. and Su, W. (2020) Pharmacokinetics and metabolism of naringin and active metabolite naringenin in rats, dogs, humans, and the differences between species. *Frontiers in Pharmacology*, **11**, 364–364.